Biomedicine & Pharmacotherapy 128 (2020) 110253

Contents lists available at ScienceDirect

Biomedicine & Pharmacotherapy

journal homepage: www.elsevier.com/locate/biopha

Original article

The effect of prolyl oligopeptidase inhibitors on alpha-synuclein aggregation and autophagy cannot be predicted by their inhibitory efficacy

Tommi P. Kilpeläinen[a], Laura Hellinen[b], Johannes Vrijdag[c], Xu Yan[d], Reinis Svarcbahs[a], Kati-Sisko Vellonen[b], Anne-Marie Lambeir[c], Henri Huttunen[d], Arto Urtti[b,e,f], Erik A.A Wallen[g], Timo T. Myöhänen[a,h,*]

[a] Drug Research Program, Division of Pharmacology and Pharmacotherapy, Faculty of Pharmacy, University of Helsinki, P.O. Box 56, 00014, Helsinki, Finland
[b] School of Pharmacy, Faculty of Health Sciences, University of Eastern Finland, 70210, Kuopio, Finland
[c] Laboratory of Medical Biochemistry and Laboratory of Medicinal Chemistry, Department of Pharmaceutical Sciences, University of Antwerp, Universiteitsplein 1, B-2610, Antwerp, Belgium
[d] Neuroscience Center, HiLIFE, University of Helsinki, P.O. Box 63, 00014, Helsinki, Finland
[e] Drug Research Program, Division of Pharmaceutical Biosciences, Faculty of Pharmacy, University of Helsinki, P.O. Box 56, FI-00014, Helsinki, Finland
[f] Laboratory of Biohybrid Technologies, Institute of Chemistry, St. Petersburg State University, Peterhof, 198504, St. Petersburg, Russia
[g] Drug Research Program, Division of Pharmaceutical Chemistry and Technology, Faculty of Pharmacy, University of Helsinki, P.O. Box 56, 00014, Helsinki, Finland
[h] Institute of Biomedicine, Integrative Physiology and Pharmacology, FI-20014, University of Turku, Turku, Finland

ARTICLE INFO

Keywords:
Serine protease
Alpha-Synuclein
Autophagy
Parkinson's disease
Protein conformation

ABSTRACT

Previous studies have shown that prolyl oligopeptidase (PREP) negatively regulates autophagy and increases the aggregation of alpha-synuclein (αSyn), linking it to the pathophysiology of Parkinson's disease. Our earlier results have revealed that the potent small molecular PREP inhibitor KYP-2047 is able to increase autophagy and decrease dimerization of αSyn but other PREP inhibitors have not been systematically studied for these two protein-protein interaction mediated biological functions of PREP. In this study, we characterized these effects for 12 known PREP inhibitors with IC_{50}-values ranging from 0.2 nM to 1010 nM. We used protein-fragment complementation assay (PCA) to assess αSyn dimerization and Western Blot of microtubule-associated protein light chain 3B II (LC3B-II) and a GFP-LC3-RFP expressing cell line to study autophagy. In addition, we tested selected compounds in a cell-free αSyn aggregation assay, native gel electrophoresis, and determined the compound concentration inside the cell by LC-MS. We found that inhibition of the proteolytic activity of PREP did not predict decreased αSyn dimerization or increased autophagy, and we also confirmed that this result did not simply reflect concentration differences of the compounds inside the cell. Thus, PREP ligands regulate the effect of PREP on autophagy and αSyn aggregation through a conformational stabilization of the enzyme that is not equivalent to inhibiting its proteolytic activity.

1. Introduction

Prolyl oligopeptidase (PREP) (EC 3.4.21.26) is a serine protease with an endopeptidase activity, cleaving peptides smaller than 30 amino acids from the carboxyl side of a proline residue [1]. PREP consists of two domains: An α/β hydrolase fold and a seven-bladed β-propeller domain which is thought to prevent larger peptides from entering the active site [2]. PREP is expressed in various tissues in both periphery and CNS, where the highest concentrations are found in the liver and testis, and in the brain cortical and nigrostriatal areas [3–5]. Even though some biologically active substrates for PREP, such as substance P, arginine-vasopressin, and thyrotropin-releasing hormone have been identified as *in vitro* PREP substrates, the physiological role of PREP is still unclear [6]. However, alterations in PREP activity have been observed in neurological conditions, such as Alzheimer's disease, Parkinson's disease, Huntington's disease, mania, clinical depression, dementia, and autism [7]. This has led to the development of small-molecular PREP inhibitors aiming to block neuropeptide catabolism.

Abbreviations: αSyn, alpha-synuclein; LC3B-II, microtubule-associated protein light chain 3B II; ZPP, *N*-benzyloxycarbonyl-L-prolyl-L-prolinal; N2A, neuro-2A neuroblastoma cells; PREP, prolyl oligopeptidase, PREP knock out HEK-293 cells, PREPko; WB, Western blot

* Corresponding author at: Division of Pharmacology and Pharmacotherapy, Drug Research Program, Viikinkaari 5E (P.O.Box 56), 00014, University of Helsinki, Finland.

E-mail address: timo.myohanen@helsinki.fi (T.T. Myöhänen).

https://doi.org/10.1016/j.biopha.2020.110253
Received 25 February 2020; Received in revised form 6 May 2020; Accepted 10 May 2020

Table 1
Tested PREP inhibitors and their IC_{50}-values against porcine PREP with references.

Compound	Structure	mol weight	LogP[b](Shake flask method)	IC_{50} (nM,pig PREP)	Reference
SUAM-1221	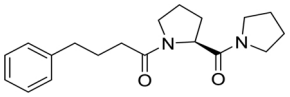	314.4290	–	2.0	Saito et al 1990 [31] Wallén et al 2002 [32]
KYP-2047	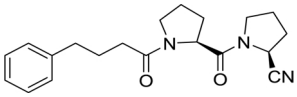	339.4412	1.6	0.2	Jarho et al 2004 [33]
KYP-2087	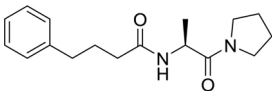	288.3910	–	147	Kilpeläinen et al 2019 [34]
KYP-2091	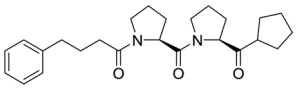	410.5580	–	1010	Wallén et al 2002 [32]
KYP-2101	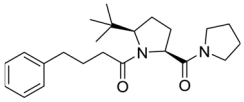	370.5730	3.3	1.2	Wallén et al 2002 [35]
KYP-2108	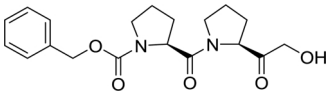	360.4100	–	0.28	Unpublished data referred to in Wallén 2003 [36]
KYP-2112	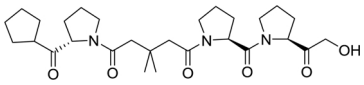	517.6600	0.7	0.32	Wallén et al 2003 [37]
KYP-2117	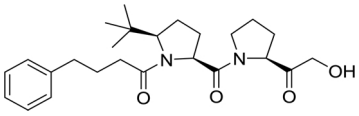	428.5730	2.3	0.26	Wallén et al 2003 [38]
KYP-2153	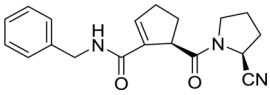	323.3960	–	0.38	Gynther et al 2004 [39]
KYP-2189	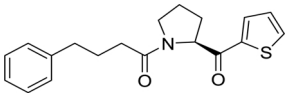	327.4420	–	3	Jarho et al 2007 [40]
ZPP	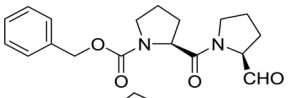	330.3840	–	0.4	Wilk et al. 1983 [26] Wallén et al 2002 [32]
S17092	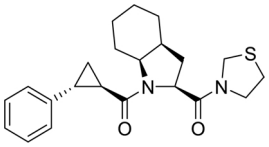	384.5830	–	1.5[a]	Barelli et al 1999 [41]

[a] K_i value against human PREP.
[b] Determined as described in Jarho et al. [33].

Although several PREP inhibitors have showed beneficial effects in preclinical memory models, and S17092, Z-321 and JTP-4819 were also tested in clinical trials as memory enhancers, their impact on neuropeptide levels remained unclear and clinical efficacy was not sufficient to support further studies [8,9].

Several functions of PREP cannot be directly linked to its proteolytic activity, for example regulation of inositol-1,4,5-triphosphate signaling [10], regulation of intracellular protein trafficking and protein secretion [11], modulation of neutrophilic inflammation [12], and neuronal cell development and differentiation [13]. This has raised interest for research into direct protein-protein interactions, and lately several interaction partners for PREP such as tubulin [11], glyceraldehyde-3-phosphate dehydrogenase [14], and growth associated protein 43 [13], have been identified. PREP has also been shown to be involved in the alpha-synuclein (αSyn) aggregation process although αSyn is not a substrate of PREP [15,16]. αSyn inclusions are connected to several neurodegenerative disorders such as Parkinson´s disease and dementia with Lewy bodies, and it also co-aggregates with Tau in Alzheimer's disease [17–19]. Inhibition of PREP with the small molecule KYP-2047 has been shown to decrease αSyn dimerization and increase autophagy, which is the main route for cells to degrade aggregated proteins *in vivo* and *in vitro*[16,20,21]. Additionally, we recently reported that PREP interacts with several proteins in the regulatory complex of protein phosphatase 2A (PP2A), including the catalytic subunit of PP2A, and that PREP inhibition or deletion activates PP2A, leading to induction of beclin-1 dependent autophagy [22]. We showed in an earlier study that PREP directly interacts with αSyn *in vitro* and in cells, and this leads to αSyn dimerization and aggregation [21]. Interestingly, the ability of PREP to increase αSyn dimerization is independent of its proteolytic activity as the proteolytically inactive S554A-PREP-mutant also

increases the dimerization of αSyn. This suggested that different PREP conformations can either induce or inhibit αSyn dimerization. PREP has at least three different conformations which are seen in native gel electrophoresis presumably representing an open, a closed, and an oligomeric form of the enzyme [23]. Moreover, it has been shown that binding of PREP inhibitor KYP-2047 stabilizes the B and His-loops of PREP which are flexible structures located near the entry site of the catalytic cavity [24]. This effect is not visible in the native gel, and there are reports showing that PREP has several conformations in dynamic equilibrium [25]. These findings indicate that certain PREP ligands could modify these protein-protein interaction mediated functions *via* conformational stabilization of the enzyme.

Typical PREP inhibitors are substrate-like peptidic compounds, *N*-benzyloxycarbonyl-L-prolyl-L-prolinal (ZPP) being the first discovered PREP inhibitor [26]. Most of the potent PREP inhibitors are based on the peptidic N-acyl-L-prolyl-pyrrolidine scaffold or they are close mimetics of it [27]. The P1 site is usually a pyrrolidine ring with an electrophilic group such as nitrile, aldehyde or hydroxyacetyl group in its 2*S*-position reacting with the nucleophilic Ser554 at the active site of PREP [28,29]. The P2 site is usually an α-aminoacyl group and P3 site is a lipophilic acyl group such as a 4-phenyl-butanoyl group. The widely used preclinical substrate-like inhibitor KYP-2047 is a slow, tight-binding inhibitor of proteolytic activity of PREP. Moreover, it has been shown to effectively enter the brain in mice when administered systematically [30]. Based on this, our research group have used KYP-2047 as a reference compound in our previous studies on αSyn aggregation and autophagy [16,20,21]. However, there are no reports where PREP inhibitors have been widely screened for their ability to decrease αSyn aggregation or to induce autophagy, and therefore, this study was undertaken to investigate how structurally diverse PREP inhibitors affect different functions of PREP.

2. Materials and methods

2.1. Chemicals and inhibitors

We selected 12 known structurally diverse PREP inhibitors (presented in Table 1), received from the old compound library from University of Kuopio (current University of Eastern Finland (UEF)). Other reagents, including ZPP (SML0205) and S-17092 (SML0181) were purchased from Sigma-Aldrich unless otherwise stated in the text.

2.2. Determination of autophagy marker LC3B-II levels

Cell culture and lysate preparation. HEK-293 cells were used throughout the experiment. Cells were obtained from ATCC (Manassas, VA) and they were authenticated by the Technology Center of Institute of Molecular Medicine Finland (FIMM, Helsinki, Finland). Cells were used at the passages 4 − 15. Cells were cultured in full Dulbecco's modified Eagle's medium (DMEM) with an additional 10% (v/v) FBS (Invitrogen), 1% (v/v) penicillin-streptomycin solution (Lonza) at 37 °C and 5% CO_2, water-saturated air. 400 000/cells per well were seeded on 6-well plates, and 24 h post plating cells were treated with tested compounds at 1 μM concentration for 4 h. After treatment, cells were lysed with mRIPA buffer (Tris − HCl 50 mM, NaCl (150 mM, 0.25% sodium deoxycholate, 1% NP-40, pH 7.4) with 1:100 protease inhibitor cocktail (Product# P8340, Sigma) and HALT phosphate inhibitor cocktail (Product# 87786, Thermo Fisher Scientific). Lysates were sonicated and centrifuged at 13,300 rpm for 15 min at 4 °C. Supernatants were collected and protein amounts were determined by the BCA method.

Western Blot (WB). The levels of autophagy markers (autophagosome marker microtubule-associated protein light chain 3B I–II (LC3BI–II)) was determined by WB as described earlier in Svarcbahs et al. [42]. Samples (20 μg protein/sample) were loaded onto a 12% polyacrylamide-SDS gel and standard transfer and blocking techniques were used. β-actin served as the loading control. Goat anti-rabbit HRP-conjugated secondary antibody (dilution 1:2000 in 5% milk; #31460, RRID:AB_228341, Thermo Fischer Scientific) was used for β-actin (dilution 1:2000 in 5% milk; ab8227, RRID:AB_2305186, AbCam) and LC3BI–II (1:1000 in 5% milk; #L7543, RRID:AB_796155, Sigma). Both antibodies gave one band corresponding to their correct molecular weight, and LC3BI-II antibody was tested with positive and negative controls in our previous study [20]. The images were captured using the C-Digit imaging system (Licor, Lincoln, USA) and 4–7 independent WB experiments were performed. Optical density (OD) of the bands were analyzed with ImageJ (histogram area analysis; version 1.48; National Institute of Health, Bethesda, MD), and the values were normalized to the loading control OD values.

2.3. Determination of autophagic flux with GFP-LC3-RFP cell line

HEK-293 cells stably expressing GFP-LC3B-RFP construct described in Kaizuka et al. [43] were created by using the protocol described in Svarcbahs et al. [22]. Shortly, HEK-293 cells were seeded at a density of 4×10^5 cells per well on 6-well plates and transfected with pMRX-IP-GFP-LC3-RFP plasmid (2500 ng/well; #84573, Addgene, Noboru Mizushima Lab; RRID:Addgene_84573) using Lipofectamine 3000 (#L3000015, ThermoFisher Scientific) transfection reagent according to the manufacturer's protocol. After 48 h, selection with 3 μg/mL puromycin cells were seeded on 96-well plates in single cell suspension, and followed based on their GFP expression. Selected cell colonies expressing GFP-LC3B-RFP were cultured further and used in experiments.

Procedure for autophagic flux determination was described in Svarcbahs et al. [22]. GFP-LC3B-RFP expressing HEK-293 cells were plated on black poly-L-lysine coated 96-well plates at a density of 35,000 cells/well. Tested compounds were used with concentration of 10 μM, rapamycin (0.5 μM; BML-A275, Enzo Life Sciences) was used as a positive control for autophagic flux induction and bafilomycin 1A (20 nM; SML1661) as an autophagy inhibitor. At 24 h post treatment, cells were washed twice with warm PBS and GFP signal was read by Victor2 multilabel counter (PerkinElmer; excitation/emission 485 nm/535 nm). For each experimental condition, 4 replicate wells were used in each experiment, and at least 3 independent experiments were performed.

Only GFP signal was used in the analysis since RFP signal was not reliably detectable in well-plate format (see supplementary Table S1 and Fig. S1), and in this construct RFP may also be degraded by lysosomes to a certain extent [43]. Representative pictures from GFP-LC3-RFP expressing cells were taken by Leica DMi8 fluorescence microscope (Leica Microsystems, Wetzlar, Germany).

2.4. Native gel electrophoresis

For detection of PREP conformations, native gel electrophoresis was used as described earlier in Savolainen et al. 2015 [21]. Briefly, 10% separating gel (40% acrylamide/bis 2.5 mL, H_2O 4.8 mL 1.5 M Tris-HCl pH 7.9, 2.5 mL, 10% SDS, 100 μL, 10% ammonium persulfate, 50 μL, TEMED, 10 μL) with stacking gel (40% acrylamide/bis, 334 μL, H_2O, 2.1 mL, 0.5 M Tris-HCl pH 6.8, 830 μL, 20% SDS 33 μL, 10% ammonium persulfate 13.5 μL, TEMED 6.5 μL) were casted, and the samples containing 0.5 μg of purified porcine recombinant PREP (purified as described in Venäläinen et al. [44]) and 1 μM concentration of PREP inhibitor diluted in native sample buffer (#1610738, Biorad). Samples were incubated for 30 min in 25 °C and 15 μL were loaded on a native gel. After electrophoresis, the gel was stained with Coomassie blue (0.1% Coomassie Blue R250, 45% ethanol and 10% glacial acetic acid) for 2 h in room temperature and destained (45% methanol, 10% glacial acetic acid) for 2 × 30 min to get a clear background before it was scanned.

2.5. Protein-fragment complementation assay (PCA) for αSyn dimerization

Cell Culture and Transfection. Mouse Neuro-2A (N2A) neuroblastoma cells and PREP knock out HEK-293 (PREPko) cells were used in the Protein-Fragment Complementation Assay (PCA). N2A cells were chosen based on their neuronal background, and HEK-293 PREPko cells were used based on their better transfectability and availability. N2A cells were obtained and authenticated by ATCC, and cultured in full Dulbecco's modified Eagle's medium (DMEM) with an additional 10% (v/v) FBS (Invitrogen), 1% (v/v) L-glutamine-penicillin-streptomycin solution (Lonza) at 37 °C and 5% CO_2. PREPko cells were generated by CRISPR-Cas9 plasmid targeted to the 3rd exon of the PREP gene as described in Svarcbahs et al. [42] and were cultured in Dulbecco's modified Eagle's medium (DMEM) with an additional 20% (v/v) FBS (Invitrogen), 1% (v/v) L-glutamine-penicillin-streptomycin solution (Lonza). Cells were used in passages 4–15. Transfection was done using JetPei (Polyplus) for N2A cells and Lipofectamine 3000 (#L3000015, ThermoFisher Scientific) for PREP-KO cells according to the manufacturer's instructions.

Plasmids. The split Gaussia princeps luciferase (GLuc) reporter plasmids and hPREP expression plasmid used in this study were previously described in Savolainen et al. [21]. All GLuc constructs used in this study have the GLuc reporter fragment placed at the N-terminus of αSyn separated by a $(GGGGS)_2SG$ linker.

PCA. PCA was performed as previously described in Savolainen et al. with small modifications [21]. N2A or PREPko cells were plated on poly-L-lysine-coated 96-well plates (PerkinElmer Life Sciences, white wall) at a density of 10,000 cells per well. 24 h post-plating, PCA reporter plasmids αSyn-GLuc1 (25 ng/well) and αSyn-GLuc2 (25 ng/well) were transfected together with or without (PREPko cells) non-tagged human PREP expression plasmid (50 ng/well; Savolainen et al. [20]).Lactacystin (10 μM, AG Scientific) was used as a positive control. PCA signal was read at 48 h post-transfection. Cells were treated with test compounds at 10 μM concentration in phenol red-free DMEM (Invitrogen) for 4 h before reading the luminescence. The PCA signal was detected by injecting 25 μL of native coelenterazine (Nanolight Technology) per well (final concentration of 20 μM), and the emitted luminescence was read using Varioskan Flash multiplate reader (Thermo Scientific). For each experimental condition, 4 replicate wells were used in each experiment, and 3–4 independent experiments with N2A cells and 2–4 with PREPko cells were performed.

2.6. αSyn in vitro aggregation assay

2.6.1. Proteins

A plasmid containing the human PREP cDNA in the pOT7_hPREP vector (IMAGE: 3614248) was obtained from GE Dharmacon (Diegem, Belgium). The coding sequence was PCR cloned in pET-46 Ek/LIC (Novagene, Madison, WI, USA) with an N-terminal hexahistidine tag using standard techniques. Human PREP was expressed in BL21(DE3) cells and purified using immobilized Co-chelating chromatography (GE Healthcare, Diegem, Belgium) followed by anion exchange chromatography on a 1 mL Mono-Q column (GE Healthcare). αSyn was expressed and purified as described by Gerard et al. 2006 [45].

2.6.2. Measurements

Sample consisted of 98 μM αSyn, 25 nM PREP, 1 μM PREP inhibitor, and 50 μM Thioflavin T in 100 μL buffer (20 mM HEPES, pH 7.40, 150 mM NaCl, 1 mM DTT) containing 0.1% (v/v) DMSO. The amounts of αSyn and PREP were based on characterization done in Brandt et al. 2008 [15] that showed that even lower amounts of PREP induce αSyn aggregation. PREP inhibitors were pre-incubated with PREP for 15 min at room temperature. Control samples, not containing PREP inhibitor and/or PREP, were also included in the experiment. After carefully covering the microtiterplate with a transparent sealing film to prevent evaporation, the sample was placed in the microtiterplate reader (Tecan Infinite M200, Tecan Group Ltd.) at 37 °C and shaken (orbital, amplitude 3.5 mm, 200 rpm, 10 s). Shaking was continued for 999 s followed by an absorbance reading (350 nm) and fluorescence reading (Ex/Em 446 nm/482 nm, gain 100 and 80, 40 flashes). The turbidity and fluorescence course were monitored kinetically every 20 min during 200 h. Magellan software was used to process the experimental data.

2.6.3. Data analysis

All experiments were performed with 6 replicates, except for the experiments containing an inhibitor but no PREP, which were performed with 3 replicates. The average, minimum, and maximum values of every experiment were used. Due to the higher robustness of the fluorescence time course compared to absorbance time course during the experiments, the fluorescence time course (gain 80) was chosen for further analysis. The fluorescence time course, emerging from the binding of thioflavin T to β-fibrils, is a measure of αSyn β-fibrils formation.

2.7. Determination of the unbound partition coefficient (Kp_{uu})

The unbound partition coefficient (Kp_{uu}) was determined with the method published previously in other cell models [46–50]. This parameter describes the ratio of unbound drug inside the cells and in the cell exterior, providing a tool to evaluate the intracellular drug exposure. The parameter is also sometimes referred to as intracellular bioavailability (F_{ic}).

The unbound partition coefficient Kp_{uu} was determined with the equation below:

$$Kp\text{uu} = Kp \times f\,\text{u, cell}$$

Where Kp is the cellular accumulation ratio at steady-state, and $f_{u,\ cell}$ is the intracellular unbound fraction.

The steady-state cellular accumulation ratio (Kp) was determined by exposing the mouse N2A cells with 0.5 μM of the PREP inhibitor in HBSS-Hepes (pH 7.4) for 4 h (at 37 °C). The cells were sub-cultured onto 48 well plates 24 h prior to the drug exposure. After 4 h of compound exposure, the medium was collected, and the intracellular drug was extracted with 60:40 acetonitrile-H_2O solution (ACN-H_2O) containing the internal standard (diclofenac), by incubation at room temperature for 15 min. The medium samples were diluted 1:10 before the analysis, with the 60:40 ACN-H_2O solution containing the internal standard (diclofenac). The protein amounts in representative cell wells were determined with the BCA protein assay.

The cellular accumulation ratio (Kp) was calculated with the following equation:

$$Kp = \frac{\frac{A\text{cell}}{V\text{cell}}}{C\text{medium}}$$

In which the A_{cell} is the intracellular drug amount, V_{cell} is the volume of the cells (calculated with 6.5 μL/mg protein) [48,51] and C_{medium} is the compound concentration in the medium.

The intracellular unbound compound fraction ($f_{u,\ cell}$) was determined with a dialysis method using Rapid Equilibrium Dialysis inserts (Thermo Fischer Scientific), and dialyzing the compounds in cell lysate for 4 h. The compounds were dialyzed as a cassette, at concentration of 0.5 μM each. The $f_{u,\ homogenate}$ was determined with the equation below:

$$f\,\text{u, homogenate} = \frac{C\text{buffer}}{C\text{homogenate}}$$

Where C_{buffer} is the concentration of the compound in the buffer chamber and the $C_{homogenate}$ is the compound concentration in the homogenate chamber. Both samples were treated with either blank cell homogenate or HBSS-Hepes buffer in order to obtain uniform matrix for the LC–MS/MS analysis. The samples were diluted with 60:40 ACN-H_2O

solution containing the internal standard (diclofenac) for the LC–MS/MS analysis.

The intracellular unbound fraction ($f_{u,cell}$) was calculated with the following equation:

$$f\,\mathrm{u,\,cell} = \frac{1}{D \times \left(\frac{1}{f\,\mathrm{u,\,homogenate}} - 1\right) + 1}$$

Where $f_{u,\ homogenate}$ is the unbound fraction in the homogenate (as described above) and the D is a dilution factor, calculated with the equation below:

$$D = \frac{1000}{Proteinconcentration\left(\frac{mg}{ml}\right) \times 6.5\left(\frac{\mu g}{ml}\right)protein}$$

2.8. Determination of compound concentrations

The compound concentrations in cell lysates were determined with liquid chromatography (Agilent 1290 with Agilent Poroshell 120 SB-C18 (2.1 × 50 mm, 2.7 μm) column) and a triple-quadrupole mass spectrometry (Agilent 6495; Agilent Technologies, Inc.) using electrospray ionization. The LC–MS/MS conditions are described in Table 2. Diclofenac was used as an internal standard in all samples.

2.9. Statistical analysis

Data are expressed as mean values ± standard error of the mean (mean ± SEM), and negative control average was set as 100% on each assay to reduce variability between repeats. Error bars in the figures represent SEM if not otherwise stated in the figure legend. Differences between groups were analyzed using 1-way ANOVA with Dunnett´s multiple comparisons post-tests. For N2A cells, αSyn dimerization PCA two-tailed unpaired student's *t*-test compared to DMSO control was used due the large number of treatment groups. In all cases, p values of < 0.05 were considered to be significant. Statistical analysis was performed using PRISM GraphPad statistical software (version 6.07, GraphPad Software, Inc., San Diego, CA).

3. Results

3.1. Effect of PREP inhibitors on autophagy and correlation to conformational changes of PREP on native gel

To investigate how different PREP inhibitors induce autophagy, we measured cellular levels of LC3B-II, an autophagosome marker, using WB (Fig. 1A**).** We have earlier shown that pharmacological inhibition or genetic ablation of PREP induces autophagic flux [20,42], and therefore, LC3B-II levels were used as an indicator of increased autophagy. The most robust increase in LC3B-II levels were seen with compounds KYP-2091 (104 % increase to DMSO control, p = 0.002, 1-way ANOVA with Dunnett´s multiple comparison), KYP-2047 (89 % increase to DMSO control, p = 0.001, 1-way ANOVA with Dunnett´s multiple comparison) and KYP-2189 (86 % increase to DMSO control, p = 0.0017, 1-way ANOVA with Dunnett´s multiple comparison) (Fig. 1A). KYP-2101, KYP-2108 and KYP-2112 did not have an effect on LC3B-II levels. Other studied compounds had an increasing trend on LC3B-II levels from 40% to 61% compared to DMSO treated control cells, but no statistical significance was found (Fig. 1A).

As LC3B-II alone is not sufficient to conclude if autophagic flux has changed [52] we used GFP-LC3-RFP expressing HEK-293 cells to monitor autophagic flux [43]. After 24 h 10 μM treatment with PREP inhibitors, no accumulation of LC3B-II vesicles were observed and most of the compounds induced a small decrease in GFP signal (Fig. 1B). KYP-2047 and KYP-2091 that showed the most potent increase in LC3B-II in WB, caused 11% and 9% decrease, respectively, in fluorescence signal compared to DMSO control (Fig. 1B). When this is combined with LC3B-II data, our results indicate increased autophagic flux after 24 h.

Since the IC_{50} value of a given compound did not predict impact on autophagic flux, we wanted to test the effect of PREP inhibitors on PREP conformations in native gel to see if weak and potent hydrolytic inhibitors can cause different conformational changes. Our results show that the potent inhibitors with IC_{50} lower than 100 nM locked PREP into one conformation but weaker inhibitors with IC_{50} higher than 100 nM did not show the same effect (Fig. 1C). However, conformational change did not correlate with the effects on LC3B-II levels in the autophagy assay.

3.2. Effect of PREP inhibitors on αSyn dimerization

To investigate the effect of different PREP inhibitors on dimerization of αSyn, a live-cell αSyn dimerization PCA was used (Fig. 2). When PREP was not overexpressed in N2A cells luminescence signal was only 41% of DMSO control ($p < 0.0001$, t = 21.75, df = 4, Student's *t*-test) (Fig. 2A), and therefore, PREP overexpression was used with N2A cells in this assay. Of the studied compounds, six were able to decrease formation of αSyn dimers in the PCA. The most potent compound in this assay was KYP-2047 with 25% reduction of luminescence signal (p = 0.0001, t = 5.45, df = 12, Student's *t*-test). Compounds SUAM-1221, KYP-2087, KYP-2091, KYP-2108 and KYP-2117 decreased αSyn dimerization 12–17% compared to the control cells. Compounds KYP-2101, KYP-2153, KYP-2189, ZPP and S17092 were not able to reduce αSyn dimerization in the PCA. To ensure that the observed effect was PREP-mediated, we treated PREPko cells for 4 h with 10 μM concentration of PREP inhibitors (Fig. 2B). No change in luminescence signal was observed. Lactacystin (luminescence signal 160% compared to DMSO control, 1-way ANOVA with Dunnett´s multiple comparisons, p = 0.0044) and 50 ng/well PREP transfection (blank) was used as a positive control for αSyn dimerization. However, when PREP was restored with transfection, the αSyn dimerization reducing effect was seen with KYP-2091 (luminescence signal 72% from DMSO control, 1-way ANOVA with Dunnett´s multiple comparisons, p = 0.0097) and KYP-2047 (luminescence signal 89% from DMSO control, not significant). Interestingly, KYP-2112 caused a small increasing effect on αSyn dimerization in this assay (luminescence signal 125% compared to DMSO control, 1-way ANOVA with Dunnett´s multiple comparisons, p = 0.028).

3.3. Effect of PREP inhibitors on αSyn aggregation in a cell-free assay

Based on the αSyn dimerization assay results, we investigated how selected PREP inhibitors with distinct structures and IC_{50} values, KYP-2047, KYP-2112 and KYP-2091, modulated αSyn aggregation in a cell-

Table 2
The mass spectrometry conditions for compound quantification.

Compound	Parent m/z	Capillary voltage (V)	Fragmentor voltage (V)	Daughter m/z (quantifier)	Daughter m/z (qualifier)	Ionization mode	Linear range
2047	340.2	3500	380	243.8	70.2	ESI +	0.1 – 500 nM
2112	518.3	3500	380	292.1	351.1	ESI +	0.1 – 500 nM
2091	411.3	3500	380	244.0	70.0	ESI +	0.1 – 500 nM
Diclofenac	296	3500	380	214	250	ESI +	n.a.

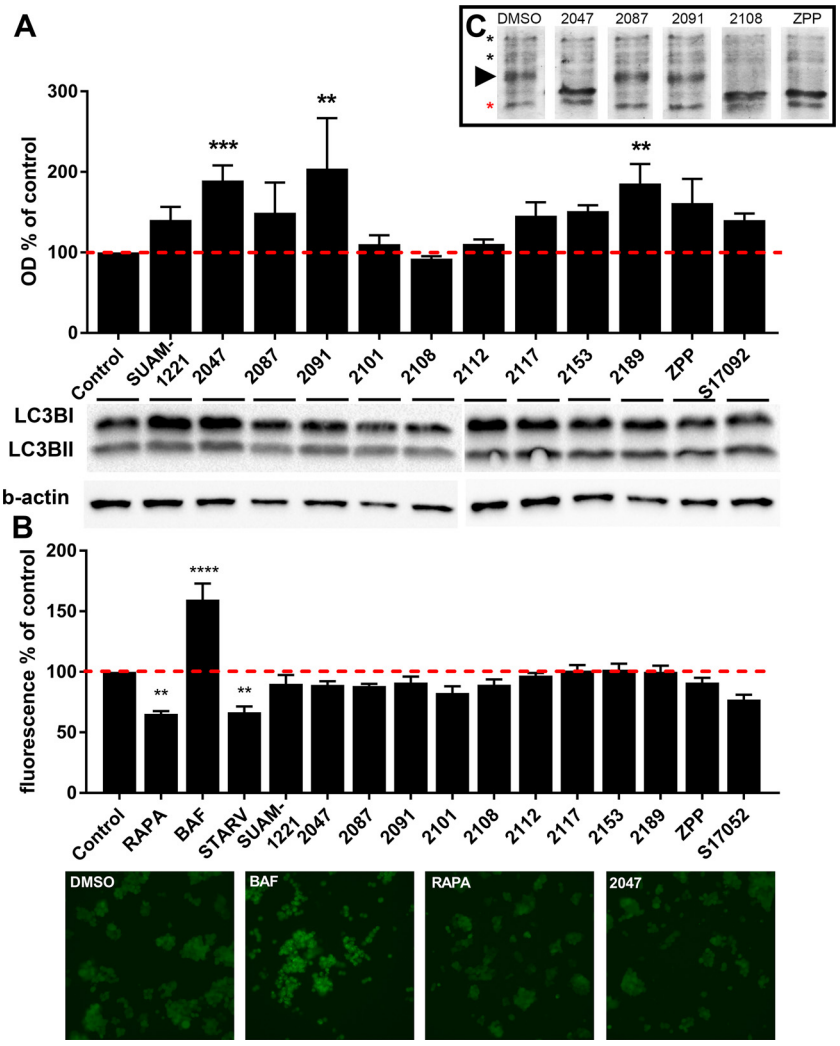

Fig. 1. The effect of PREP inhibitors on autophagy. **(A)** The effect of tested PREP inhibitors on LC3B-II levels in HEK-293 cells at 1 μM concentration and with 4 h treatment. KYP-2047, KYP-2091 and KYP-2189 had statistically significant increases in the levels of LC3B-II: 189%, 204%, and 186 %, respectively, compared to DMSO control. Data is presented as mean + SEM (n = 3-7), 1-way ANOVA with Dunnett´s multiple comparison to DMSO control, ** $p < 0.05$, *** $p < 0.001$. Full images of blots are shown in Supplementary Fig. S1. **(B)** The effect of 24 h 10 μM treatment of studied PREP inhibitors on autophagic flux in GFP-LC3-RFP expressing HEK-293 cells. None of the tested PREP inhibitors showed accumulation of LC3-II protein whereas 20 nM bafilomycin 1A (BAF) increased accumulation of LC3B and inhibited autophagic flux. 500 nM rapamycin (RAPA) treatment and serum starvation (STARV) induced autophagic flux significantly even after 24 h treatment. Data are presented as mean + SEM (n = 3-12), 1-way ANOVA with Dunnett´s multiple comparison to DMSO control, ** $p < 0.005$, *** $p < 0.001$, **** $p < 0.0001$. Hatched red line indicates the level of DMSO control. **(C)** Native gel conformation of recombinant human PREP protein in the presence of selected PREP inhibitors. Potent inhibitors KYP-2047, KYP-2108 and ZPP changed the equilibrium of PREP conformations, but weaker inhibitors KYP-2087 and KYP-2091 did not show such a change. Black arrowhead represents dominant conformation of PREP, black stars represent minor conformations of PREP, and the red star represents an unspecific band seen in all treatments.

free assay. Interestingly, unlike in the PCA, all tested inhibitors reversed the accelerating effect of PREP on αSyn aggregation (Fig. 3). However, there was no difference between a weak enzymatic inhibitor (KYP-2091) and strong inhibitors (KYP-2112 and KYP-2047) of the proteolytic activity in this assay, although the concentration used in this assay (1 μM) is at the IC_{50} value of KYP-2091 (1010 nM; Table 1; Fig. 3). Similar to Brandt et al. [15], PREP accelerated the spontaneous αSyn aggregation process (β-fibril formation) but at the endpoint, the overall aggregation was higher without PREP (Fig. 3). As the assay was not performed using aSyn and PREP inhibitors in absence of PREP, we cannot fully exclude the direct impact of PREP inhibitors on aSyn fibrillization.

3.4. Determination of the unbound partition coefficient (Kp_{uu})

To explain the differences in αSyn PCA and *in vitro* aggregation assays, and why a less potent PREP inhibitor (KYP-2091) outperforms several potent inhibitors in our assays, we next investigated if there was a difference in cellular penetration of the compounds. To assess the free concentration inside the cell, we determined the unbound partition coefficient (Kp_{uu}) for compounds KYP-2047, KYP-2112 and KYP-2091. All studied PREP inhibitors showed similar Kp_{uu} values (Fig. 4C) ranging from 0.9 to 1.9.

4. Discussion

Previous studies have shown that PREP inhibition by KYP-2047 decreases αSyn aggregation and induces autophagy [16,21], and this contributes to decreased αSyn levels and toxicity in cells and *in vivo* [20]. However, this is the first study where a structurally diverse set of PREP inhibitors were characterized against αSyn aggregation and as autophagy inducers.

The studied compounds are inhibitors of the proteolytic activity of PREP with IC_{50} values ranging from 0.2 nM to 1010 nM but our results showed that their effects on the other functions of PREP, αSyn dimerization and autophagy marker LC3B-II upregulation, did not correlate with the IC_{50} values. Interestingly, the weakest inhibitor of the proteolytic activity tested in the current study, KYP-2091 with an IC_{50}-value of 1010 nM, had a clear effect on autophagy and on αSyn dimerization in the cellular assays. On the other hand, the potent inhibitors for proteolytic activity, KYP-2101 and KYP-2112 with IC_{50}-values of 1.2 and 0.32 nM, respectively, effected neither αSyn dimerization nor LC3-II levels in the autophagy assay. These findings are in line with our recent study, where we showed that PREP ligands having a tetrazole group at the P1 site and IC_{50}-values ranging from 12 to even 200 000 nM had a reducing effect on αSyn dimerization in PCA, while more potent PREP inhibitors did not show the same effect [34]. Importantly, the results with αSyn dimerization and the autophagy assays suggest that different inhibitors may bind differently on PREP, causing variable changes to PREP structures that regulate protein-protein interactions. To support this hypothesis, our previous molecular docking studies suggested that PREP ligands with a tetrazole group bind differently to the active site of the enzyme [34].

As KYP-2047 is the only compound of tested inhibitors that has been

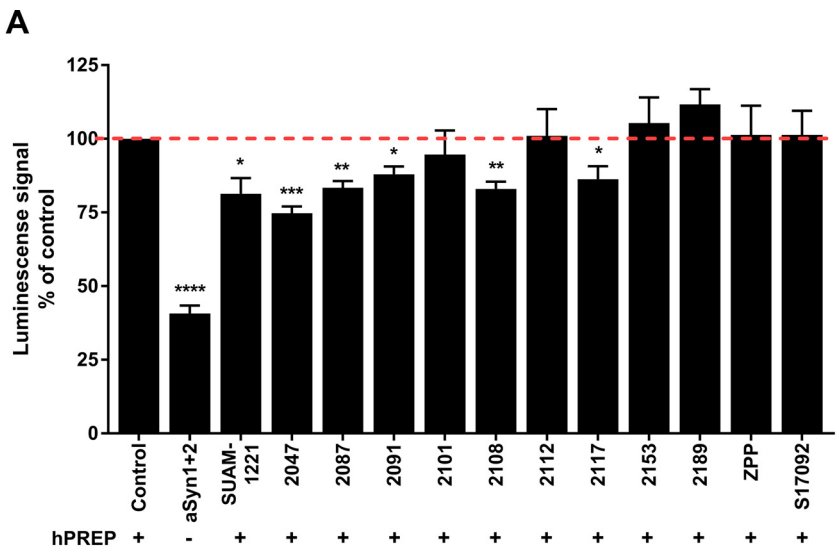

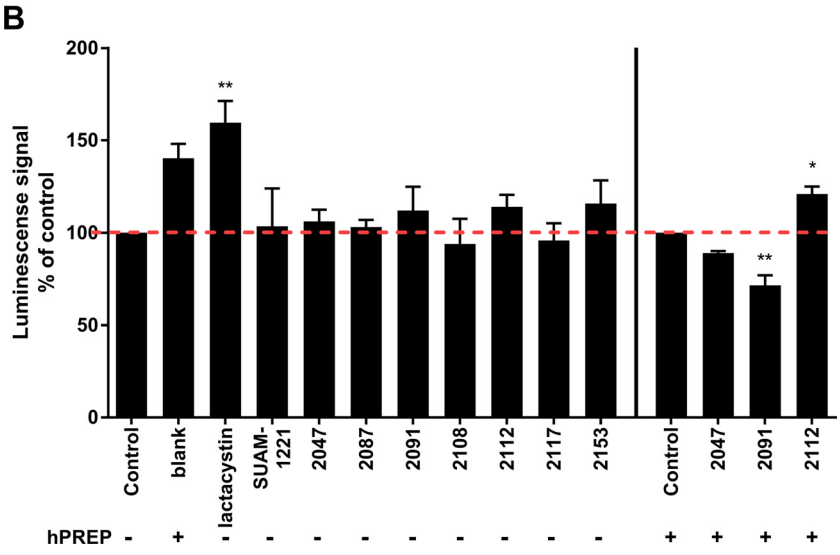

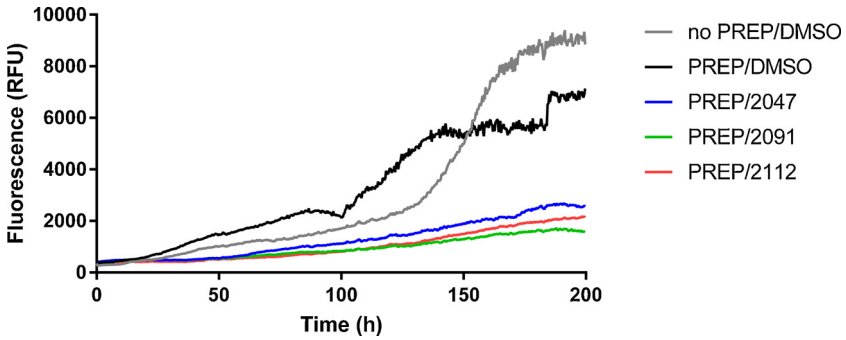

Fig. 2. The effect of PREP inhibitors on αSyn dimerization. **(A)** αSyn dimerization in N2A cells as determined by protein-fragment complementation assay (PCA) with PREP over-expression (PREP inhibitors added at 10 μM final concentration for 4 h). Compounds SUAM-1221, KYP-2047, KYP-2087, KYP-2091, KYP-2108 and KYP-2117 reduced the amount of αSyn1-αSyn2 interaction 12-25% of control. KYP-2047 showed the most potent effect on αSyn dimerization with 25% reduction, while KYP-2091 being the least potent with 12% reduction in αSyn dimerization. αSyn1 + αSyn2 + mock cells served as a negative control for αSyn dimerization as there is no PREP overexpression. Data are presented as mean + SEM, (n = 3-11), (*** $p < 0.001$, ** $p < 0.01$, * $p < 0.05$; Student´s *t*-test compared to DMSO control). **(B)** αSyn dimerization in PREPko cells. No effect with PREP inhibitors were observed when PREP was not present in the cells. Transfection of hPREP increased αSyn dimerization and PREP inhibitor KYP-2047 (not statistically significant) and KYP-2091 were able to decrease this compared to DMSO control. Data are presented as mean + SEM, 1-way ANOVA with Dunnett´s multiple comparison to DMSO control, * $p < 0.05$, ** $p < 0.005$. Hatched red line indicates the level of DMSO control.

Fig. 3. Impact of PREP inhibitors αSyn aggregation *in vitro*. αSyn aggregation assay (β-sheet formation followed by Thioflavin-T) was performed in the presence or absence of PREP and PREP inhibitors in a cell-free assay.

under off-target analysis [53], we cannot fully exclude off-target effects of give inhibitors. However, our results with the αSyn dimerization assay in PREPko cells showed that the impact of PREP inhibitors on αSyn dimerization are PREP-related. Additionally, our earlier results with PREP knock-out cells show that removal of PREP indeed induces autophagic flux, and our recent study showed that this is related to interaction based regulation of PREP on PP2A [20,22]. Differences in cellular penetration of the compounds could possibly explain the results. To study this, we selected KYP-2047, KYP-2091, and KYP-2112 for Kp_{uu} assay to determine the unbound partition coefficient, and our results showed that these results could not be explained by differences in intracellular drug exposure. The unbound partition coefficient (Kp_{uu}) is a relevant parameter to evaluate intracellular drug exposure, as it describes the ratio of free drug inside the cells and in the cell exterior [47–50]. As lower cellular accumulation was coupled with higher $f_{u,cell}$ and *vice versa* the parameter describing the free drug exposure (Kp_{uu}) is similar among all of the studied PREP inhibitors. This indicates that in the case of these PREP inhibitors, similar free drug amount is available

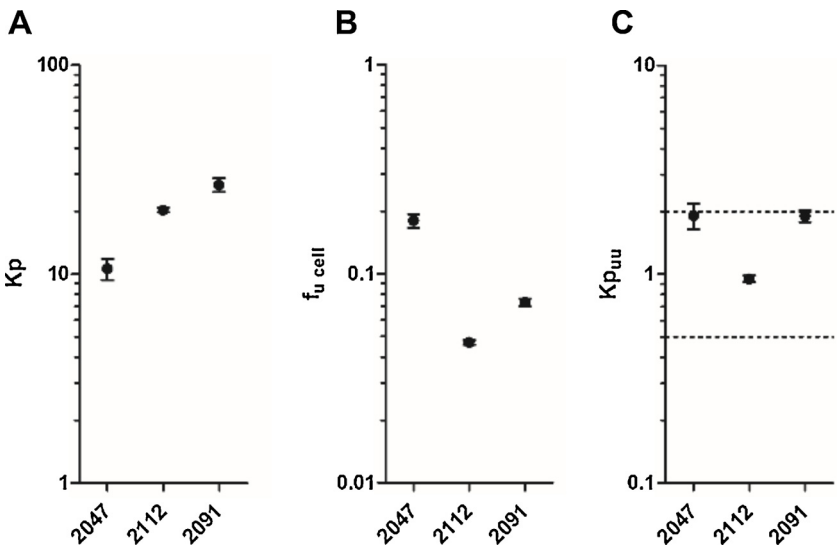

Fig. 4. The intracellular drug exposure of PREP inhibitors KYP-2047, KYP-2112 and KYP-2091 is similar. The unbound partition coefficient (Kp_{uu}) is ranging from 0.9 to 1.9 (**C**). The range of Kp_{uu} values in which the passive permeation is expected to dominate the equilibrium (0.5 − 2) is marked with dotted lines. Error bars represent ± SEM.

inside the cells to bind to the target, when the exposure concentration is equal. The determined Kp_{uu} values were in the range of 0.9–1.9, indicating that passive permeation across the plasma membrane dominates the equilibrium, and active processes (active transport, metabolism) or intracellular sequestration (*e.g.* lysosomotropism) are not significantly altering the cellular kinetics of these compounds.

The *in vitro* αSyn aggregation assay showed that all studied compounds: KYP-2047, KYP-2091, and KYP-2112 prevented the formation of αSyn fibrils similar to Brandt et al. 2008 [15]. This is slightly controversial compared to the αSyn PCA results but notably, compound KYP-2091, with an IC_{50} value that is over 1000-fold higher compared to IC_{50} values of other tested compounds, had the best impact on reversing the αSyn aggregation in the cell-free assay. The concentration of PREP inhibitors used in the measurements were 1000 nM which means that with KYP-2091 approximately 50% of the PREP still had proteolytic activity. This indicates that the magnitude of inhibition of PREP's proteolytic activity does not correlate directly with the reduction of αSyn aggregation in the cell-free assay. Interestingly, compound KYP-2112 was not able to decrease αSyn dimerization in the αSyn PCA, but decreased the aggregation *in vitro*. This might be due to a significantly more complex environment in the cell-based model.

As stated above, we suggest that different biological activity profiles by different PREP inhibitors is most likely resulting from differences in how the bound PREP ligands stabilize or allow certain flexibility of the conformation of the enzyme, especially the loops around the active site. The hypothesis is that the required conformation of the enzyme is not equivalent for an effect of PREP on autophagy, αSyn aggregation, and proteolytic activity. Our view is supported by our previous study, where we showed that a mutation in external loop B at the surface of PREP (T590C) removed the inhibitory activity of PREP on PP2A [22]. The native gel assay showed that conformational changes of PREP is in line with the IC_{50}-value of tested compounds as small molecules having an IC_{50} lower than 10 nM changed the equilibrium of conformations. However, the changes seen in the native gel did not follow the autophagy induction or αSyn dimerization reducing effect. Changes in native gel conformations are likely to be more drastic compared to the subtle movements of PREP loops which might modulate protein-protein interactions [24]. This is supported by the multiple quantum relaxation dispersion assay where ZPP and KYP-2047 gave slightly different spectra on PREP even though they are both potent inhibitors and have the same effect on the native gel [54]. There are also other reports where potent inhibitors of PREP proteolytic activity have different biological effects. For example, KYP-2047 and SUAM-14746 had a different impact on trophoblast stem cell differentiation [55] and that weak PREP inhibitors are able to decrease the amount of mutant αSyn in neuroblastoma cells [56]. Therefore, the effect of different PREP ligands on the PREP conformation requires detailed protein structure studies.

Our study shows that ligands with a close structural similarity to SUAM-1221 (the inhibitor having only the 4-phenylbutanoyl-L-prolyl-pyrrolidine backbone) are preferred for the αSyn dimerization reducing effect. However, introduction of an electrophile at the P1 site seems to change the situation slightly. For example, ZPP, with a formyl group at the P1 site, was not able to decrease αSyn dimerization whereas KYP-2108 with a hydroxyacetyl group in the same position had an effect on αSyn dimerization. A more reactive electrophilic group is likely to anchor it strongly to the active site of the enzyme and thereby decreasing the opportunity for alternative binding modes, which may affect the conformational flexibility of PREP. The nitrile in KYP-2047, hydroxyacetyl in KYP-2108, and ketone in KYP-2091 are less reactive electrophiles than an aldehyde in ZPP indicating that a too strong electrophile might not be preferable. This is supported by the fact that compounds SUAM-1221 and KYP-2087 lacking the electrophile has a reducing effect on αSyn dimerization in the PCA. On the other hand, adding an electrophile in some scaffolds might lead to a decreasing effect on αSyn dimerization in PCA as seen when comparing compounds KYP-2101 and KYP-2117.

In conclusion, PREP ligands are likely to regulate the effect of PREP on autophagy and αSyn aggregation through a conformational stabilization of the enzyme that is not equivalent to inhibiting its proteolytic activity. From the perspective of drug discovery, it would be beneficial to develop PREP ligands with an increased selectivity towards the autophagy inducing effect and/or αSyn dimerization reducing effect. However, the exact mechanisms by which small molecular compounds regulate these protein-protein interaction mediated functions of PREP need to be studied further for better understanding of the decoupled structure-activity relationships that we have revealed in this study.

Author contributions

TK, XY, RS performed PCA, WB, autophagy cell line and native gel studies, and HH provided constructs and expertise for PCA study. LH performed the intracellular drug concentration assay, and KSV performed the LC–MS/MS analysis and AU contributed expertise and infrastructure for these assays. JV purified αSyn and performed the *in vitro* aggregation assay. AML provided proteins, expertise and infrastructure for the *in vitro* aggregation assay. TTM, EW, AU, HJH and AML designed the study and all authors contributed to the writing and

editing of the manuscript.

Declaration of Competing Interest

The authors declare that they have no known competing financial interests or personal relationships that could have appeared to influence the current study.

Acknowledgements

The authors want to thank Professor Seppo Auriola (University of Eastern Finland) for advice on LC–MS/MS analysis. Johannes Vrijdags is a post-doctoral fellow of the Research Foundation - Flanders (FWO). The work was supported by grants from Academy of Finland (grants 303833, 305710, 267788, and 273799), University of Helsinki 3-year grant, Jane and Aatos Erkko Foundation, Sigrid Juselius Foundation and HiLife proof-of-concept grant for TTM and by an Academy of Finland (grant 296409) for HJH.

Appendix A. Supplementary data

Supplementary material related to this article can be found, in the online version, at doi:https://doi.org/10.1016/j.biopha.2020.110253.

References

[1] L. Polgár, The prolyl oligopeptidase family, Cell. Mol. Life Sci. 59 (2) (2002) 349–362.
[2] V. Fülöp, Z. Böcskei, L. Polgár, Prolyl oligopeptidase: an unusual ß-propeller domain regulates proteolysis, Cell 94 (2) (1998) 161–170.
[3] F.H. Goossens, I. De Meesler, G. Vanhoofand, S. Schärpe, Distribution of prolyl oligopeptidase in human peripheral tissues and body fluids, Eur. J. Clin. Chem. Clin. Biochem. 34 (1) (1996) 17–22.
[4] T.T. Myöhänen, J.I. Venäläinen, J.A. García-Horsman, M. Piltonen, P.T. Männistö, Distribution of prolyl oligopeptidase in the mouse whole-body sections and peripheral tissues, Histochem. Cell Biol. 130 (5) (2008) 993–1003.
[5] T.T. Myöhänen, J.I. Venäläinen, E. Tupala, J.A. Garcia-Horsman, R. Miettinen, P.T. Männistö, Distribution of immunoreactive prolyl oligopeptidase in human and rat brain, Neurochem. Res. 32 (8) (2007) 1365–1374.
[6] J.A. García-Horsman, P.T. Männistö, J.I. Venäläinen, On the role of prolyl oligopeptidase in health and disease, Neuropeptides 41 (1) (2007) 1–24.
[7] I. Brandt, S. Scharpé, A.M. Lambeir, Suggested functions for prolyl oligopeptidase: a puzzling paradox, Clin. Chim. Acta 377 (1-2) (2007) 50–61.
[8] P.T. Männisto, J. Vanäläinen, A. Jalkanen, J.A. García-Horsman, Prolyl oligopeptidase: a potential target for the treatment of cognitive disorders, Drug News Perspect. 20 (5) (2007) 293–305.
[9] R. Svarcbahs, U. Julku, T. Kilpeläinen, M. Kyyrö, M. Jäntti, T.T. Myöhänen, New tricks of prolyl oligopeptidase inhibitors – a common drug therapy for several neurodegenerative diseases, Biochem. Pharmacol. 161 (2019) 113–120.
[10] A.J. Harwood, Prolyl oligopeptidase, inositol phosphate signalling and lithium sensitivity, CNS Neurol. Disord. - Drug Targets 10 (3) (2011) 333–339.
[11] I. Schulz, U. Zeitschel, T. Rudolph, D. Ruiz-Carrillo, J.U. Rahfeld, B. Gerhartz, V. Bigl, H.U. Demuth, S. Roßner, Subcellular localization suggests novel functions for prolyl endopeptidase in protein secretion, J. Neurochem. 94 (4) (2005) 970–979.
[12] M.A. Roda, M. Sadik, A. Gaggar, M.T. Hardison, M.J. Jablonsky, S. Braber, J.E. Blalock, F.A. Redegeld, G. Folkerts, P.L. Jackson, Targeting prolyl endopeptidase with valproic acid as a potential modulator of neutrophilic inflammation, PLoS One 9 (5) (2014).
[13] E. Di Daniel, C.P. Glover, E. Grot, M.K. Chan, T.H. Sanderson, J.H. White, C.L. Ellis, K.T. Gallagher, J. Uney, J. Thomas, P.R. Maycox, A.W. Mudge, Prolyl oligopeptidase binds to GAP-43 and functions without its peptidase activity, Mol. Cell. Neurosci. 41 (3) (2009) 373–382.
[14] T. Matsuda, M. Sakaguchi, S. Tanaka, T. Yoshimoto, M. Takaoka, Prolyl oligopeptidase is a glyceraldehyde-3-phosphate dehydrogenase-binding protein that regulates genotoxic stress-induced cell death, Int. J. Biochem. Cell Biol. 45 (4) (2013) 850–857.
[15] I. Brandt, M. Gérard, K. Sergeant, B. Devreese, V. Baekelandt, K. Augustyns, S. Scharpé, Y. Engelborghs, A.M. Lambeir, Prolyl oligopeptidase stimulates the aggregation of a-synuclein, Peptides 29 (9) (2008) 1472–1478.
[16] T.T. Myöhänen, M.J. Hannula, R. Van Elzen, M. Gerard, P. Van Der Veken, J.A. García-Horsman, V. Baekelandt, P.T. Männistö, A.M. Lambeir, A prolyl oligopeptidase inhibitor, KYP-2047, reduces a-synuclein protein levels and aggregates in cellular and animal models of Parkinson's disease, Br. J. Pharmacol. 166 (3) (2012) 1097–1113.
[17] M.G. Spillantini, M. Goedert, The a-synucleinopathies: parkinson's disease, dementia with Lewy bodies, and multiple system atrophy, Ann. N. Y. Acad. Sci. 920 (2000) 16–27.
[18] N. Badiola, R.M. de Oliveira, F. Herrera, C. Guardia-Laguarta, S.A. Gonçalves, M. Pera, M. Suárez-Calvet, J. Clarimon, T.F. Outeiro, A. Lleó, Tau enhances α-synuclein aggregation and toxicity in cellular models of synucleinopathy, PLoS One 6 (10) (2011).
[19] X. Yan, R.L. Uronen, H.J. Huttunen, The interaction of α-synuclein and Tau: A molecular conspiracy in neurodegeneration? Semin. Cell Dev. Biol. (2018).
[20] M.H. Savolainen, C.T. Richie, B.K. Harvey, P.T. Männistö, K.A. Maguire-Zeiss, T.T. Myöhänen, The beneficial effect of a prolyl oligopeptidase inhibitor, KYP-2047, on alpha-synuclein clearance and autophagy in A30P transgenic mouse, Neurobiol. Dis. 68 (2014) 1–15.
[21] M.H. Savolainen, X. Yan, T.T. Myöhänen, H.J. Huttunen, Prolyl oligopeptidase enhances a-Synuclein dimerization via direct protein-protein interaction, J. Biol. Chem. 290 (8) (2015) 5117–5126.
[22] R. Svarcbahs, M. Jяантti, T. Kilpelяинen, U.H. Julku, L. Urvas, S. Kivioja, S. Norrbacka, T.T. Myяяhяянen, Prolyl oligopeptidase inhibition activates autophagy via protein phosphatase 2A, Pharmacol. Res. (2020) 151.
[23] Z. Szeltner, T. Juhász, I. Szamosi, D. Rea, V. Fülöp, K. Módos, L. Juliano, L. Polgár, The loops facing the active site of prolyl oligopeptidase are crucial components in substrate gating and specificity, Biochimica et Biophysica Acta (BBA) - Proteins Proteomics 1834 (1) (2013) 98–111.
[24] A. Tsirigotaki, R. Van Elzen, P. Van Der Veken, A.M. Lambeir, A. Economou, Dynamics and ligand-induced conformational changes in human prolyl oligopeptidase analyzed by hydrogen/deuterium exchange mass spectrometry, Sci. Rep. 7 (1) (2017).
[25] N. Kichik, T. Tarragó, B. Claasen, M. Gairí, O. Millet, E. Giralt, 15N relaxation NMR studies of prolyl oligopeptidase, an 80 kDa enzyme, reveal a pre-existing equilibrium between different conformational states, ChemBioChem 12 (18) (2011) 2737–2739.
[26] S. Wilk, M. Orlowski, Inhibition of rabbit brain prolyl endopeptidase by N-Benzyloxycarbonyl-Prolyl-Prolinal, a transition state aldehyde inhibitor, J. Neurochem. 41 (1) (1983) 69–75.
[27] J. Lawandi, S. Gerber-Lemaire, L. Juillerat-Jeanneret, N. Moitessier, Inhibitors of prolyl oligopeptidases for the therapy of human diseases: defining diseases and inhibitors, J. Med. Chem. 53 (9) (2010) 3423–3438.
[28] K. Kaszuba, T. Róg, R. Danne, P. Canning, V. Fülöp, T. Juhász, Z. Szeltner, J.F. St. Pierre, A. García-Horsman, P.T. Männistö, M. Karttunen, J. Hokkanen, A. Bunker, Molecular dynamics, crystallography and mutagenesis studies on the substrate gating mechanism of prolyl oligopeptidase, Biochimie 94 (6) (2012) 1398–1411.
[29] P. Van Der Veken, V. Fülöp, D. Rea, M. Gerard, R. Van Elzen, J. Joossens, J.D. Cheng, V. Baekelandt, I. De Meester, A.M. Lambeir, K. Augustyns, P2-substituted N-acylprolylpyrrolidine inhibitors of prolyl oligopeptidase: biochemical evaluation, binding mode determination, and assessment in a cellular model of synucleinopathy, J. Med. Chem. 55 (22) (2012) 9856–9867.
[30] A.J. Jalkanen, J.V. Leikas, M.M. Forsberg, KYP-2047 penetrates mouse brain and effectively inhibits mouse prolyl oligopeptidase, Basic Clin. Pharmacol. Toxicol. 114 (6) (2014) 460–463.
[31] M. Saito, M. Hashimoto, N. Kawaguchi, H. Fukami, T. Tanaka, N. Higuchi, Synthesis and inhibitory activity of acylpeptidyl-prolinal derivatives toward post-proline cleaving enzyme as nootropic agents, J. Enzyme Inhib. Med. Chem. 3 (3) (1990) 163–178.
[32] E.A.A. Wallén, J.A.M. Christiaans, S.M. Saario, M.M. Forsberg, J.I. Venäläinen, H.M. Paso, P.T. Männistö, J. Gynther, 4-Phenylbutanoyl-2(S)-acylpyrrolidines and 4-phenylbutanoyl-L-prolyl-2(S)-acylpyrrolidines as prolyl oligopeptidase inhibitors, Bioorg. Med. Chem. 10 (7) (2002) 2199–2206.
[33] E.M. Jarho, J.I. Venäläinen, J. Huuskonen, J.A.M. Christiaans, J.A. Garcia-Horsman, M.M. Forsberg, T. Järvinen, J. Gynther, P.T. Männistö, E.A.A. Wallén, A cyclopent-2-enecarbonyl group mimics proline at the P2 position of prolyl oligopeptidase inhibitors, J. Med. Chem. 47 (23) (2004) 5605–5607.
[34] Tommi P. Kilpeläinen, J. K. T, Maija K. Lahtela-Kakkonen, Tony S. Eteläinen, Timo T. Myöhänen, Erik A.A. Wallén, The Effect of 4-phenylbutanoyl-aminoacyl-2(S)-tetrazolylpyrrolidines on the Functions of Prolyl Oligopeptidase, Submitted manuscript (2019).
[35] E.A.A. Wallén, J.A.M. Christiaans, M.M. Forsberg, J.I. Venäläinen, P.T. Männistö, J. Gynther, Dicarboxylic acid bis(L-prolyl-pyrrolidine) amides as prolyl oligopeptidase inhibitors, J. Med. Chem. 45 (20) (2002) 4581–4584.
[36] E.A.A. Wallén, Desing and Synthesis of Novel Prolyl Oligopeptidase Inhibitors, University of Kuopio, Kuopio University Publications A., 2003.
[37] E.A.A. Wallén, J.A.M. Christiaans, E.M. Jarho, M.M. Forsberg, J.I. Venäläinen, P.T. Männistö, J. Gynther, New prolyl oligopeptidase inhibitors developed from dicarboxylic acid bis(L-prolyl-pyrrolidine) amides, J. Med. Chem. 46 (21) (2003) 4543–4551.
[38] E.A.A. Wallén, J.A.M. Christiaans, T.J. Saarinen, E.M. Jarho, M.M. Forsberg, J.I. Venäläinen, P.T. Männistö, J. Gynther, Conformationally rigid N-acyl-5-alkyl-L-prolyl-pyrrolidines as prolyl oligopeptidase inhibitors, Bioorg. Med. Chem. 11 (17) (2003) 3611–3619.
[39] J. Gynther, P.T. Männistö, E. Wallén, H. Christaans, M. Forsberg, A. Poso, J. Venäläinen, E. Helkala, Compounds Having Prolyl Oligopeptidase Inhibitory Activity, WO 2004/060862 A3 (2004).
[40] E.M. Jarho, J.I. Venäläinen, S. Poutiainen, H. Leskinen, J. Vepsäläinen, J.A.M. Christiaans, M.M. Forsberg, P.T. Männistö, E.A.A. Wallén, 2(S)-(Cycloalk-1-enecarbonyl)-1-(4-phenyl-butanoyl)pyrrolidines and 2(S)-(aroyl)-1-(4-phenylbutanoyl)pyrrolidines as prolyl oligopeptidase inhibitors, Bioorg. Med. Chem. 15 (5) (2007) 2024–2031.
[41] H. Barelli, A. Petit, E. Hirsch, S. Wilk, G. De Nanteuil, P. Morain, F. Checler, S 17092-1, a highly potent, specific and cell permeant inhibitor of human proline

endopeptidase, Biochem. Biophys. Res. Commun. 257 (3) (1999) 657–661.
[42] R. Svarcbahs, U.H. Julku, S. Norrbacka, T.T. Myöhänen, Removal of prolyl oligopeptidase reduces alpha-synuclein toxicity in cells and in vivo, Sci. Rep. 8 (1) (2018).
[43] T. Kaizuka, H. Morishita, Y. Hama, S. Tsukamoto, T. Matsui, Y. Toyota, A. Kodama, T. Ishihara, T. Mizushima, N. Mizushima, An autophagic flux probe that releases an internal control, Mol. Cell 64 (4) (2016) 835–849.
[44] J.I. Venäläinen, R.O. Juvonen, M.M. Forsberg, A. Garcia-Horsman, A. Poso, E.A.A. Wallen, J. Gynther, P.T. Männistö, Substrate-dependent, non-hyperbolic kinetics of pig brain prolyl oligopeptidase and its tight binding inhibition by JTP-4819, Biochem. Pharmacol. 64 (3) (2002) 463–471.
[45] M. Gerard, Z. Debyser, L. Desender, P.J. Kahle, J. Baert, V. Baekelandt, Y. Engelborghs, The aggregation of alpha-synuclein is stimulated by FK506 binding proteins as shown by fluorescence correlation spectroscopy, FASEB J. 20 (3) (2006) 524–526.
[46] A. Mateus, P. Matsson, P. Artursson, A high-throughput cell-based method to predict the unbound drug fraction in the brain, J. Med. Chem. 57 (7) (2014) 3005–3010.
[47] A. Mateus, A. Treyer, C. Wegler, M. Karlgren, P. Matsson, P. Artursson, Intracellular drug bioavailability: a new predictor of system dependent drug disposition, Sci. Rep. (2017) 7.
[48] A. Treyer, A. Mateus, J.R. Wiśniewski, H. Boriss, P. Matsson, P. Artursson, Intracellular drug bioavailability: effect of neutral lipids and phospholipids, Mol. Pharm. 15 (6) (2018) 2224–2233.
[49] A. Mateus, L.J. Gordon, G.J. Wayne, H. Almqvist, H. Axelsson, B. Seashore-Ludlow, A. Treyer, P. Matsson, T. Lundbäck, A. West, M.M. Hann, P. Artursson, Prediction of intracellular exposure bridges the gap between target- and cell-based drug discovery, Proc. Natl. Acad. Sci. U.S.A. 114 (30) (2017).
[50] A. Treyer, M. Ullah, N. Parrott, B. Molitor, S. Fowler, P. Artursson, Impact of intracellular concentrations on metabolic drug-Drug interaction studies, AAPS J. 21 (5) (2019).
[51] C.M. Gillen, B. Forbush Iii, Functional interaction of the K-Cl cotransporter (KCC1) with the Na-K- Cl cotransporter in HEK-293 cells, Am. J. Physiol. - Cell Physiol. 276 (2 45-2) (1999) C328–C336.
[52] D.J. Klionsky, K. Abdelmohsen, et al., Guidelines for the Use and Interpretation of Assays for Monitoring Autophagy, 3rd edition, (2020), pp. 1554–8635 (Electronic).
[53] A.J. Jalkanen, T.P. Piepponen, J. Hakkarainen, I. J.; De Meester, A.M. Lambeir, M.M. Forsberg, The effect of prolyl oligopeptidase inhibition on extracellular acetylcholine and dopamine levels in the rat striatum, Neurochem. Int. 60 (3) (2012) 301–309.
[54] A. López, F. Herranz-Trillo, M. Kotev, M. Gairí, V. Guallar, P. Bernadó, O. Millet, T. Tarragó, E. Giralt, Active-site-Directed inhibitors of prolyl oligopeptidase abolish its conformational dynamics, ChemBioChem 17 (10) (2016) 913–917.
[55] Y. Maruyama, S. Matsubara, A.P. Kimura, Mouse prolyl oligopeptidase plays a role in trophoblast stem cell differentiation into trophoblast giant cell and spongiotrophoblast, Placenta 53 (2017) 8–15.
[56] R. Kumar, R. Bavi, M.G. Jo, V. Arulalapperumal, A. Baek, S. Rampogu, M.O. Kim, K.W. Lee, New compounds identified through in silico approaches reduce the a-synuclein expression by inhibiting prolyl oligopeptidase in vitro, Sci. Rep. 7 (1) (2017).